Chinese Chemical Letters 36 (2025) 110053

Contents lists available at ScienceDirect

Chinese Chemical Letters

journal homepage: www.elsevier.com/locate/cclet

Targeting TRPA1 with liposome-encapsulated drugs anchored to microspheres for effective osteoarthritis treatment

Yulin Chen[a,b,1], Guangchao Wang[a,1], Fengjin Zhou[c,1], Zhifeng Yin[d,1], Fuming Shen[e,f,g], Weizong Weng[e], Hao Zhang[a,e], Yingying Jiang[e,f,g], Xinru Liu[e,f,g], Yonghui Deng[h], Yuan Chen[b,*], Ke Xu[e,f,g,i,*], Jiacan Su[a,e,f,g,*]

[a] Department of Orthopedics, Xinhua Hospital, Shanghai Jiao Tong University School of Medicine, Shanghai 200092, China
[b] Department of Orthopedics and Traumatology, Nanning Hospital of Traditional Chinese Medicine, Guangxi University of Chinese Medicine, Nanning 530200, China
[c] Department of Orthopedics, Honghui Hospital, Xi'an Jiaotong University, Xi'an 710000, China
[d] Department of Orthopedics, Shanghai Zhongye Hospital, Shanghai 200444, China
[e] Institute of Translational Medicine, Shanghai University, Shanghai 200444, China
[f] Organoid Research Center, Shanghai University, Shanghai 200444, China
[g] National Center for Translational Medicine (Shanghai) SHU Branch, Shanghai University, Shanghai 200444, China
[h] Department of Chemistry, Department of Gastroenterology, Zhongshan Hospital of Fudan University, State Key Laboratory of Molecular Engineering of Polymers, Fudan University, Shanghai 200433, China
[i] Wenzhou Institute of Shanghai University, Wenzhou 325000, China

ARTICLE INFO

Article history:
Received 17 February 2024
Revised 23 May 2024
Accepted 24 May 2024
Available online 26 May 2024

Keywords:
Microsphere
HAMA hydrogel
Liposome
Osteoarthritis
TRPA1

ABSTRACT

Crucial for mediating inflammation and the perception of pain, the ion channel known as transient receptor potential ankyrin 1 (TRPA1) holds significant importance. It contributes to the increased production of cytokines in the inflammatory cells of cartilage affected by osteoarthritis and represents a promising target for the treatment of this condition. By leveraging the unique advantages of liposomes, a composite microsphere drug delivery system with stable structural properties and high adaptability can be developed, providing a new strategy for osteoarthritis (OA) drug therapy. The liposomes as drug reservoirs for TRPA1 inhibitors were loaded into hyaluronic acid methacrylate (HAMA) hydrogels to make hydrogel microspheres *via* microfluidic technology. An *in vitro* inflammatory chondrocyte model was established with interleukin-1β (IL-1β) to demonstrate HAMA@Lipo@HC's capabilities. A destabilization of the medial meniscus (DMM) mouse model was also created to evaluate the efficacy of intra-articular injections for treating OA. HAMA@Lipo@HC has a uniform particle-size distribution and is injectable. The drug encapsulation rate was 64.29% $\pm$ 2.58%, with a sustained release period of 28 days. Inhibition of TRPA1 *via* HC-030031 effectively alleviated IL-1β-induced chondrocyte inflammation and matrix degradation. In DMM model OA mice, microspheres showed good long-term sustained drug release properties, improved joint inflammation microenvironment, reduced articular cartilage damage and decreased mechanical nociceptive threshold. This research pioneers the creation of a drug delivery system tailored for delivery into the joint cavity, focusing on TRPA1 as a therapeutic target for osteoarthritis. Additionally, it offers a cutting-edge drug delivery platform aimed at addressing diseases linked to inflammation.

The global burden of osteoarthritis (OA) is increasing due to an aging population, rising obesity rates, and frequent joint injuries, with an estimated 527.81 million people affected worldwide [1]. During the early stages of OA, the synovial and cartilage tissues within the joint exhibit substantial production of pro-inflammatory factors, notably interleukin (IL)-1, IL-6, IL-8, and transforming growth factor-β (TGF-β). This heightened production subsequently triggers increased chondrocyte apoptosis, elevated synthesis of matrix metalloproteinases (MMPs), and the degradation of the extracellular matrix (ECM) [2]. Consequently, a compromised matrix that cannot endure normal mechanical stress forms, ultimately leading to joint destruction [3,4]. In this process, there are interactions between cartilage, sclerosis, and synovium, which

* Corresponding authors.
E-mail addresses: Cheny2801@163.com (Y. Chen), kexu@shu.edu.cn (K. Xu), drsujiacan@163.com (J. Su).
[1] These authors contributed equally to this work.

https://doi.org/10.1016/j.cclet.2024.110053
1001-8417/

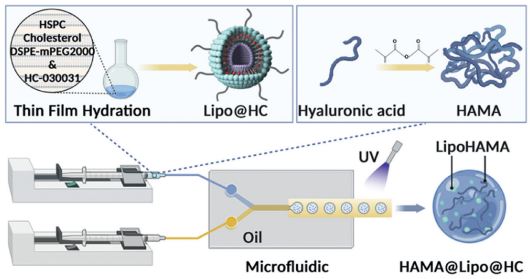

Scheme 1. The principle and fabrication of HAMA@Lipo@HC, and design of the composite microspheres for treating osteoarthritis by anti-inflammatory and regulating matrix degradation. Created with BioRender.com.

will further amplify the tissue damage [5,6]. Hence, it becomes apparent that inflammation significantly contributes to the progression of the disease, underscoring the importance of research aimed at the early phases of OA [7]. In current clinical practice, pharmacological interventions are commonly used to alleviate initial arthritis symptoms and prevent progression [8]. Traditional OA drugs, plagued by poor solubility and low bioavailability, require frequent, higher dosing, potentially causing gastrointestinal and organ damage [9-11]. Overcoming these treatment challenges remains a key clinical focus. Transient receptor potential ankyrin 1 (TRPA1) is a non-selective cation channel protein, which is involved in pain and inflammation [12,13]. It has been revealed that intervention on TRPA1 can effectively inhibit tissue inflammation, and cartilage degradation, which is a potential drug target for the treatment of OA [14-16]. HC-030031, a selective TRPA1 blocker with hydrophobic properties like traditional osteoarthritis drugs, requires high and frequent dosing for effectiveness [17,18]. Enhancing drug pharmacokinetics through improved dosage forms is a key research focus to address these challenges [19].

Nanoparticles in drug delivery systems are gaining attention for treating OA, offering reduced dosages, fewer administrations, increased efficacy, and lower toxicity [20,21]. Liposomes (Lipo) are amphiphilic nano-drug carriers that encapsulate both hydrophilic and lipophilic drugs, known for their high drug loading, slow release, low toxicity, biocompatibility, and biodegradability, making them popular in drug carrier research [22]. Locally applied in joint cavities, they reduce drug washout by synovial fluid, extend drug duration, and improve lubrication and cartilage condition to treat OA [23,24]. Despite liposomes' advantages, their clinical use is limited by certain drawbacks, which hydrogels can offset due to their stable and adaptable properties [25]. By combining these with liposomes' benefits, composite materials that maximize both substances' strengths can be created [26].

Hyaluronic acid (HA) is crucial in cartilage's ECM, enhancing cellular function and promoting differentiation, while also regulating inflammation and tissue repair [27]. Hyaluronic acid hydrogels can be obtained by introducing methacrylic groups into HA, and their injectability and easily adjustable size give them potential as a novel delivery system [28,29]. Based on this, we synthesized a HAMA@Lipo hydrogel microsphere targeting TRPA1 (Scheme 1). The TRPA1 inhibitor was encased within the liposomes' phospholipid bilayer, synthesized through the thin film hydration technique. These liposomes were then combined with hyaluronic acid methacrylate (HAMA) to form HAMA@Lipo hydrogel microspheres utilizing a microfluidic approach [30,31]. Following their degradation, assessments of encapsulation efficiency, drug liberation, and biocompatibility were conducted. The composite microspheres' anti-inflammatory capabilities and ability to regulate matrix metabolism were confirmed in primary mouse chondrocytes. The injectable microspheres facilitated sustained drug release and exhibited effective therapeutic outcomes in a mouse model of destabilization of the medial meniscus (DMM)-induced OA.

First, we demonstrated the functional expression of TRPA1 in mice primary chondrocytes, the extraction and identification of mice primary chondrocytes as shown in Fig. S1 (Supporting information). After pharmacological inhibition by HC-030031, both gene and protein levels showed a downregulation of inflammatory factor levels, a homeostasis of cartilage matrix metabolism, and cartilage matrix staining to visualize the drug effect (Fig. S2 in Supporting information). We also performed experiments with chondrocytes that had knocked down TRPA1 expression to further validate that TRPA1 mediates chondrocyte inflammation (Fig. S3 in Supporting information). Blank liposomes were synthesized *via* a thin film hydration method with hydrogenated soybean phosphatidylcholine (HSPC), 1,2-distearoyl-*sn*–glycero-3-phosphoethanolamine-*N*-[methoxy(polyethylene glycerol)–2000] (DSPE-MPEG2000) and cholesterol, referring to our previous work [32]. As shown in Fig. 1A, liposomes present a uniform spherical shape structure by transmission electron microscope (TEM) for observing their morphology. The zeta potential of the blank liposomes was −18.2 mV, which slightly increased to −16.3 mV after drug loading, with a polydispersity (PDI) of 0.129 and a particle size of 100–120 nm, indicating that our prepared liposomes had a suitable particle size (Figs. 1B and C). HAMA@Lipo microspheres were prepared using a microfluidic device. As shown in Fig. 1D, where the microspheres (ii) prepared after mixing the liposome solution (i) with the hydrogel settled naturally at the bottom of the Eppendorf (EP) tube. Under the optical microscopy, the microspheres appeared uniformly dispersed in water, with a smooth, round morphology and an average diameter of 150 μm (Figs. 1E and F). The morphology of the microspheres after dehydration was observed *via* scanning electron microscopy (SEM), and their profiles had a clear structure of reticulated porosity, which facilitated the loading of more liposomes (Fig. 1G). The elemental composition of HAMA@Lipo was analyzed using energy dispersive X-ray (EDS), confirming the successful incorporation of phosphorus from liposomes into the hydrogel (Fig. 1H). DiI-labeled liposomes verified through laser scanning confocal microscopy (LSCM) demonstrated uniform distribution within the microspheres (Fig. 1I). HAMA@Lipo is a purely physical envelope with no new characteristic peaks formed in its Fourier transform infrared spectroscopy (FTIR), and the addition of liposomes makes the mechanical properties degrade (Figs. S4A and B in Supporting information). Combining the above characterization results, we successfully prepared HAMA@Lipo.

Using liposomes to deliver hydrophobic drugs improves their aqueous solubility and prolongs their body retention, enhancing hydrophobic drug utilization [33]. Here, we used high performance liquid chromatography (HPLC) to detect the drug loading (Fig. S5 in Supporting information), the encapsulation rate of drug-carrying liposomes obtained from the preparation was up to 86.76%, and the encapsulation rate of microspheres prepared by further mixing with HAMA was 64.29% (Fig. 2A). The decrease in HAMA@Lipo@HC encapsulation rate may be due to shear pressure in the microfluidic system causing drug leakage during preparation, and the use of organic solvents to remove paraffin oil may also contribute to this result [26]. The drug release curves were plotted for 28 days detect the drug release from liposomes and microspheres at each defined time point, as shown in Fig. 2B. The liposomes released almost all the drugs explosively within one week, compared with the significantly much slower release rate of HAMA@Lipo, where the drugs were not released abruptly but continuously under the dual blockage of liposomes and hydrogels.

An enzymatic degradation method was used to simulate the degradation of the microspheres *in vivo* to ensure that HAMA@Lipo achieves optimal drug delivery [34]. As shown in Fig. 2C, the mi-

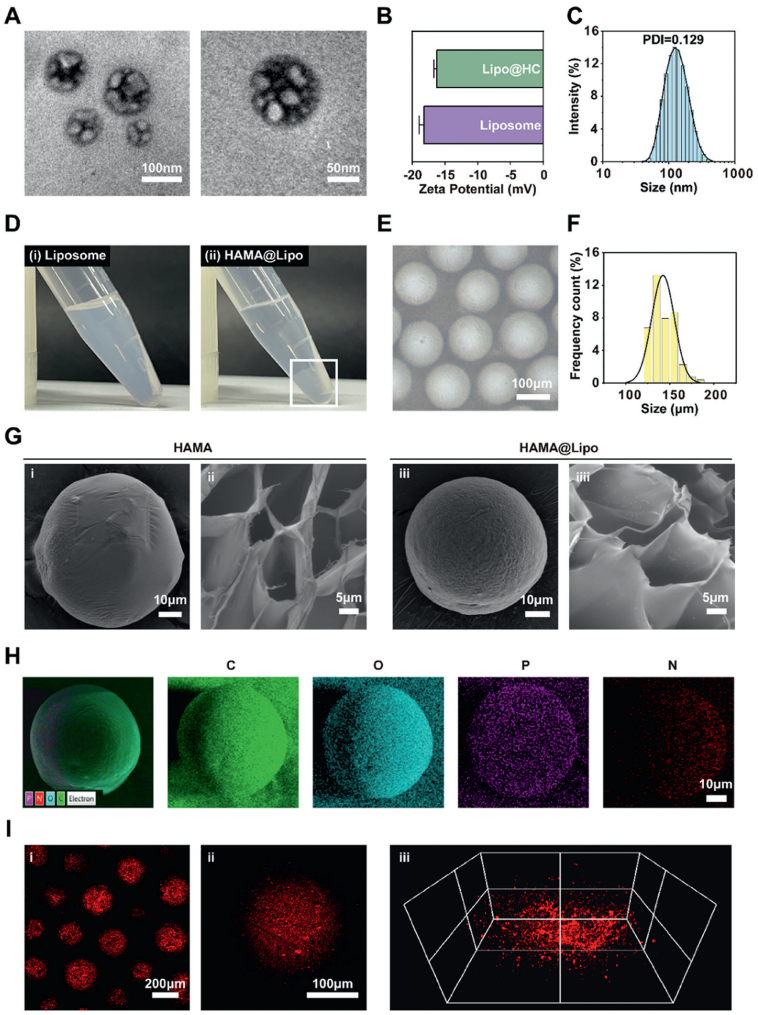

Fig. 1. Characterization of liposome and HAMA@Lipo. (A) TEM image of the liposome. (B) Zeta potential distribution of liposomes. Data are presented as mean ± standard deviation (SD) ($n = 3$). (C) Hydrodynamic diameters of liposomes. (D) (i) Liposome solution and (ii) HAMA@Lipo microspheres loaded with liposomes. (E) Microscopic images of HAMA@Lipo. (F) Particle size distribution of the microspheres ($n = 150$). (G) SEM image of HAMA and HAMA@Lipo from (i, iii) the overall view and (ii, iiii) the local view. (H) Elemental mapping images of the HAMA@Lipo. C: carbon; O: oxygen; P: Phosphorus; N: Nitrogen. (I) Images of HAMA@Lipo microspheres *via* LSCM. Liposomes in microspheres were labeled with Dil dye.

crospheres remain unchanged for the first 3 days but develop a rough surface by day 7. By day 14, cracks appear, followed by extensive disintegration by day 21, leaving only gel fragments by day 28. The microspheres were weighed on dry weight at each time point and the degradation curve is shown in Fig. 2D. The biocompatibility of HAMA@Lipo on chondrocyte viability was confirmed by Live/Dead and CCK-8 assays, and the results showed that the microspheres did not impair chondrocyte viability (Figs. 2E and F).

Patients with OA have high IL-1β levels in their cartilage and synovial fluid, and modeling OA inflammation with IL-1β increases TRPA1 expression and Ca^{2+} influx in chondrocytes [35,36]. Elevated Ca^{2+} influx through TRPA1 channels increased inflammation in chondrocytes, leading to higher MMPs (especially MMP13) and a disintegrin and metalloproteinase with thrombospondin motifs (ADAMTSs) levels, resulting in cartilage matrix degradation and production imbalance [37]. To evaluate the effect of TRPA1 inhibitor release from HAMA@Lipo on cartilage function, chondrocytes were first exposed to 10 ng/mL IL-1β for 24 h to mimic joint inflammation, then HAMA@Lipo@HC was added (Fig. 2G). The Western blot (WB) results showed that HAMA@Lipo@HC could successfully release inhibitors to reduce TRPA1 expression levels (Fig. S6A in Supporting information). Moreover, using Fluo-3-AM fluorescent dye to measure Ca^{2+} influx, IL-1β-treated chondrocytes exhibited significantly greater fluorescence, suggesting elevated Ca^{2+} influx. Conversely, the introduction of HAMA@Lipo@HC significantly reduced this fluorescence intensity (Fig. 2H). TNF-α and IL-6, traditional markers of inflammation, are found in high concentrations in the knee joints of individuals with OA [38]. As shown in Fig. S6B (Supporting information), IL-1β-stimulated chondrocyte inflammatory factor expression levels were significantly increased, HC-030031 inhibited TRPA1 thereby reducing inflammation, and the microspheres group with statistically significant differences from the blank group. Enzyme-linked immunosorbent assay (ELISA) is a common assay of detecting cytokine secretion levels, which further used to measure the levels of inflammatory factors in the chondrocyte supernatant, as shown in Fig. S6C (Supporting information). Next, Alcian blue staining visually reflected chondrogenic differentiation, and the HAMA@Lipo@HC group significantly increased the intensity of cell staining after IL-1β treatment (Fig. 3A). The WB assay results showed that IL-1β treatment increased MMP13 and decreased collagen type II (COL-II) expression in chondrocytes, which was reversed by HAMA@Lipo@HC treatment (Fig. 3B). The results of the RT-qPCR assay in Fig. 3C showed a significant increase in MMP13 and ADAMTS5 expression in the stimulated chondrocytes, and a substantial downregulation of COL-II and SOX9 expression, which are key factors for cartilage

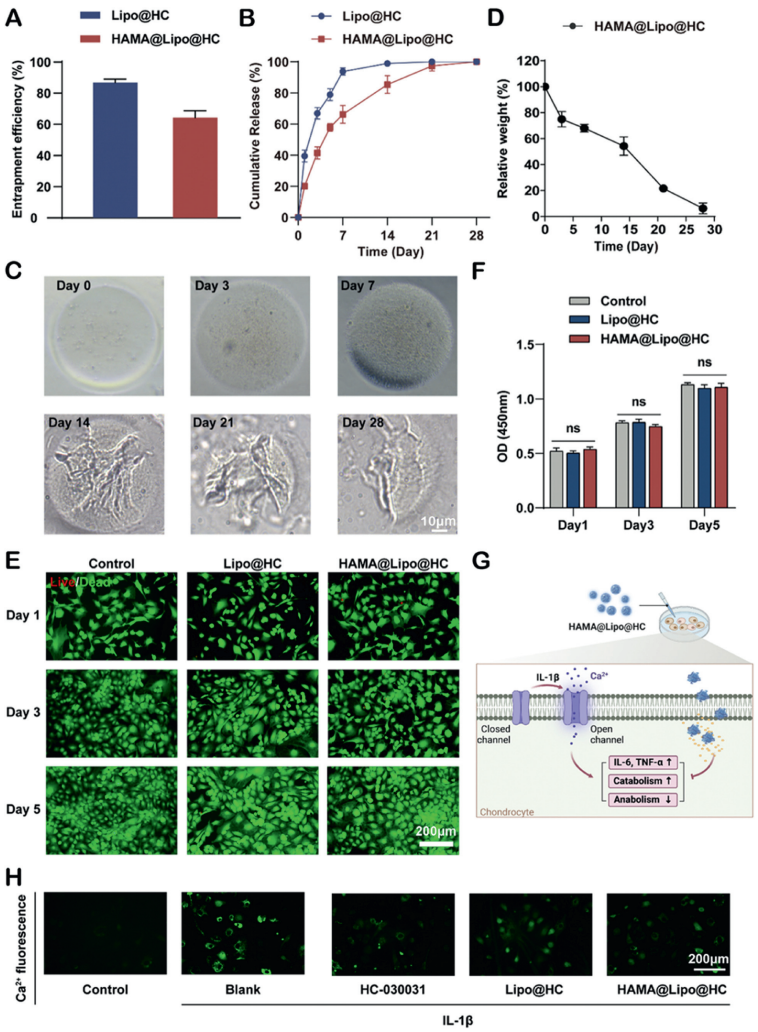

Fig. 2. Drug loading, release properties, degradation, biocompatibility and reduction of cartilage inflammation of HAMA@Lipo. (A) The encapsulation efficiency of HC-030031 in the liposome, and HAMA@Lipo. (B) Release curve of HC-030031 from liposome, and HAMA@Lipo. (C) Degradation of HAMA@Lipo microgels after treatment with 10 U/mL hyaluronidase *in vitro*. (D) The degradation curves of HAMA@Lipo. (E) Live/dead staining of chondrocytes cocultured with Lipo@HC and HAMA@Lipo@HC after 1, 3, and 5 days show the toxicity of the microsphere components. (F) The CCK-8 results on 1, 3, and 5 days. OD, optical density. (G) HAMA@Lipo@HC inhibit inflammation and cartilage degradation induced by IL-1β through inhibitor release. (H) Representative images of Ca^{2+} fluorescence in different chondrocyte treatment groups. Data are presented as mean ± SD ($n = 3$). ns, no statistically significant difference between groups.

synthesis. Immunofluorescence staining assessed MMP13 and COL-II, key cartilage biomarkers, in IL-1β-treated chondrocytes. Results showed that HAMA@Lipo@HC enhanced COL-II synthesis and reduced MMP13 activity (Figs. 3D–G). The above experimental results suggest that the HAMA@Lipo@HC possesses the ability to regulate the inflammation-substrate metabolic balance, which may be a promising therapeutic.

Experiments used 8-week-old male C57BL/6J mice (20–22 g) from Changzhou Cavens Laboratory Animal Co., treated according to Care and Use of Laboratory Animals. All animal experimental procedures were strictly conducted in accordance with the established guidelines for animal experiments and had received approval from the Animal Ethics Committee of Shanghai University (No. 2023–022). Starting four weeks post-surgery, phosphate buffered saline (PBS), HC-030031, HAMA, Lipo@HC, and HAMA@Lipo@HC were administered weekly to five of the groups, with the study concluding eight weeks after the commencement of treatments. The right knee joint and serum harvested were used for the assessment of OA treatment effects by radiography, histology, and inflammatory factor expression levels in serum (Fig. 4A). The bone density distribution of the subchondral bone will change during the development of osteoarthritis, and the subchondral bone microstructure will remodel and thicken to form dense tissue [39]. The schematic diagram of the subchondral bone was obtained through micro-computed tomography (micro-CT) tomography followed by three-dimensional (3D) reconstruction, which visualized the degree of subchondral bone sclerosis in the proximal femur (Fig. 4B). Compared with the DMM group, the subchondral bone microstructure was improved in the HC-030031 group, HAMA group, Lipo@HC group, and HAMA@Lipo@HC group, with the most pronounced effect in the HAMA@Lipo@HC. Moreover, analysis of bone volume/tissue volume (BV/TV), subchondral bone plate thickness (SBP.th), and trabecular pattern factor (Tb.pf) at the medial tibial plateau further quantified subchondral bone changes (Figs. 4C–E). HAMA@Lipo@HC is thought to have positively influenced the biomechanical characteristics and microstructure of subchondral bone during the early stages of OA.

The results of the von Frey and cold plate tests showed that pain perception significantly decreased in the second week after treatment with HAMA@Lipo@HC, and this severe pain gradually diminished with an increasing number of treatments (Figs. S7A and B in Supporting information). Subsequently, we examined al-

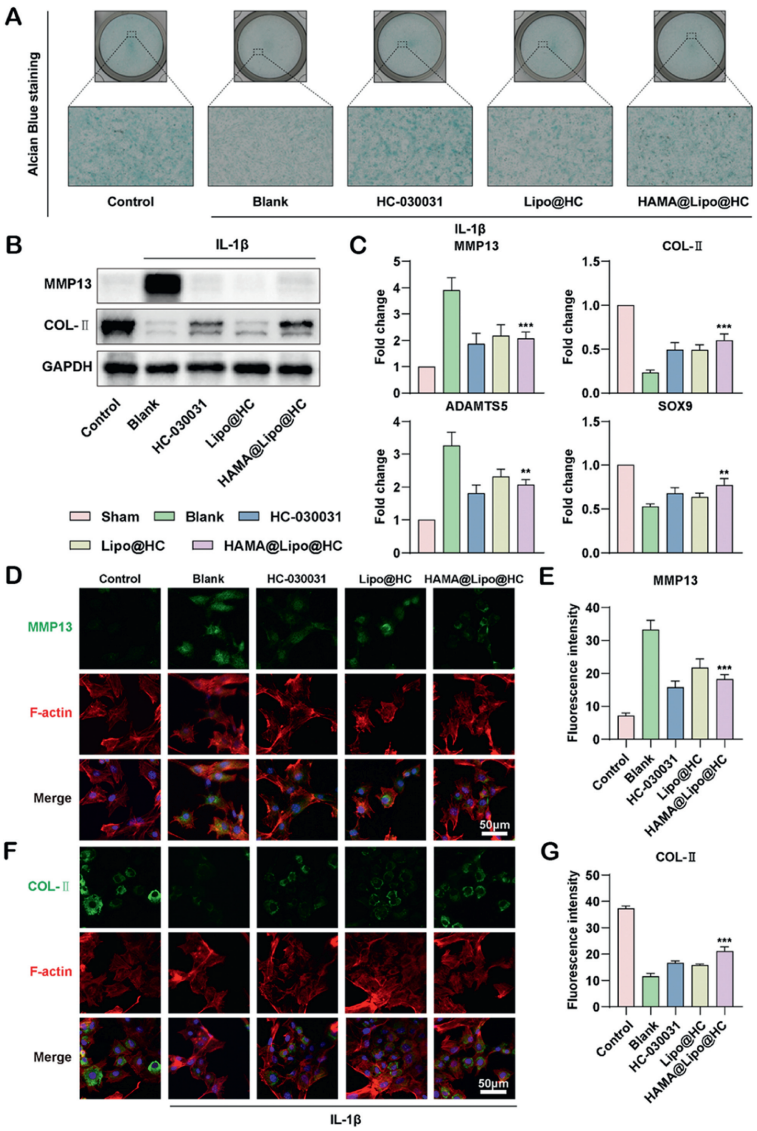

Fig. 3. Inhibition of cartilage degradation effects of HAMA@Lipo@HC. (A) Representative images of alcian blue staining of chondrocytes treated with IL-1β or IL-1β and HC-030031, liposomes or microspheres co-cultured for 24 h. (B) The protein expression level of MMP13, and COL-II. (C) The mRNA expression level of MMP13, ADAMTS5, COL-II, and Sox9. (D) The representative immunofluorescence staining results of MMP13. (E) Quantification of MMP13 fluorescence. (F) The representative immunofluorescence staining results of COL-II. (G) Quantification of COL-II fluorescence. All data were from $n = 3$ independent experiments. Data are presented as mean ± SD. $^{**}P < 0.01$, $^{***}P < 0.001$ *vs.* the Blank group.

terations in cartilage histology following microsphere treatment safranin O-fast green staining (S&F) by utilizing as well as hematoxylin and eosin (H&E) for articular cartilage (Figs. 4F and G). While, after injection of the therapeutic agent into the joint, the drug-laden hydrogel microsphere treatment group showed significant improvement in cartilage, with the joint indicating smoothness and significant cartilage staining. MMP13 expression in articular cartilage was assessed by immunohistochemistry. The Lipo@HC and HAMA@Lipo@HC groups had fewer positive cells than the PBS group, with the greatest reduction in the HAMA@Lipo@HC group (Fig. 4H). Furthermore, the HAMA@Lipo@HC group's effect on cartilage degeneration was scored by the Osteoarthritis Research Society International (OARSI) criteria, showing no significant difference from the sham group (Fig. S7C in Supporting information). To evaluate the *in vivo* anti-inflammatory effect of microsphere-delivered drugs, we analyzed the serum's inflammatory factor expression levels (Figs. S7D–F in Supporting information). Specifically, the therapeutic effect of drug-loaded microspheres was better, which is consistent with the aforementioned imaging and histological results. H&E staining revealed no significant lesions in major mouse organs or notable differences in organ appearance between groups, and biochemical markers in orbital blood samples showed no significant variations across all groups (Figs. S8 and S9 in Supporting information).

Previous studies have reported the successful development of liposome-hydrogel composite delivery systems with promising therapeutic effects [26]. In this study, based on TRPA1, a potential therapeutic target for OA, we prepared a hydrogel microsphere named HAMA@Lipo by microfluidic system, which formed by HAMA hydrogels anchored with TRPA1 inhibitor-loaded liposomes, and application for OA treatment. HAMA@Lipo exhibited good stability, biocompatibility, and its slow drug release improved drug utilization, both at the *in vitro* cellular level and *in vivo* animal level, and showed superior to the liposomes. The simple micro and minimally invasive drug delivery reduced inflammatory factor levels, regulated the metabolic balance of ECM, reduced subchon-

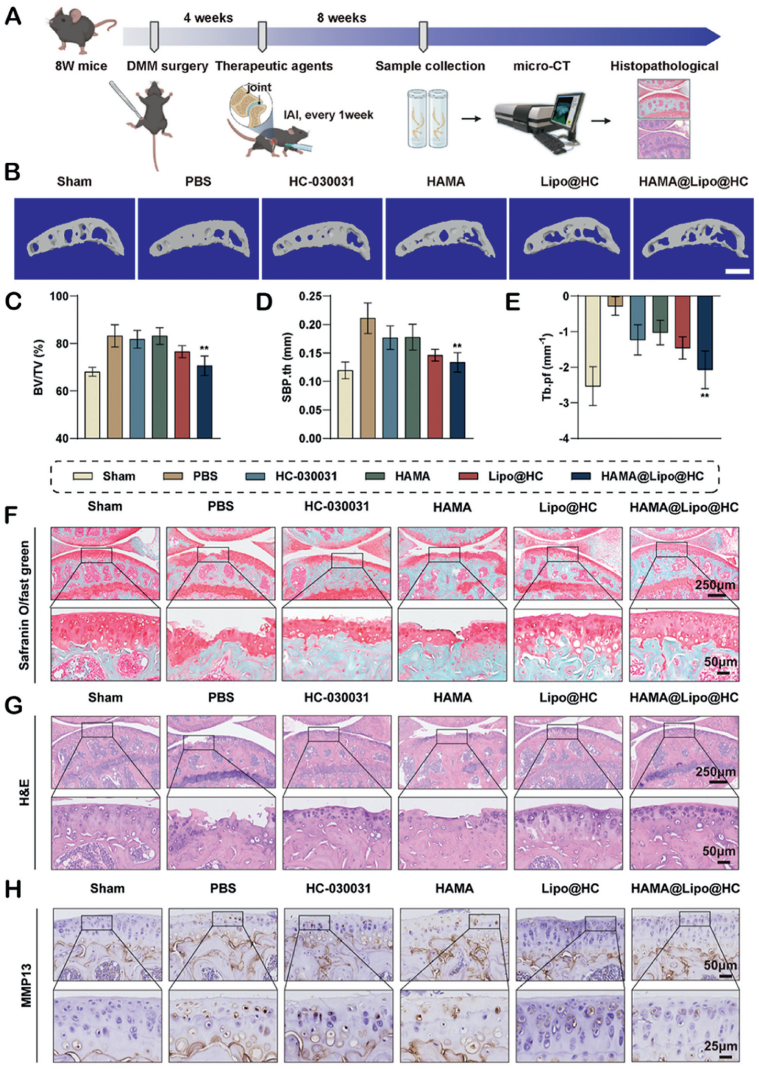

Fig. 4. Radiology, pain behavior, S&F staining, H&E staining and immunohistochemical staining. (A) Timeline of treatment and surgery. (B) Three-dimensional images of the sagittal plane of medial tibial subchondral bone structure at 12 weeks after the operation (scale bar: 100 μm). (C–E) Micro-CT quantitative analysis of tibial subchondral bone of BV/TV (%), SBP.th (mm) and Tb.pf (mm^{-1}). (F, G) Representative images of S&F staining, and H&E staining. (H) Representative images of MMP13 protein immunohistochemical staining. All data were from $n = 6$ independent experiments. Data are presented as mean ± SD. $^{**}P < 0.01$ *vs.* the PBS group.

dral osteosclerosis, and greatly reduced joint pain in mice. Overall, the HAMA@Lipo drug delivery system is an ideal delivery system that provides a new strategy for the treatment of osteoarthritis.

Declaration of competing interest

The authors declare that they have no known competing financial interests or personal relationships that could have appeared to influence the work reported in this paper.

CRediT authorship contribution statement

Yulin Chen: Writing – original draft. **Guangchao Wang:** Data curation. **Fengjin Zhou:** Software. **Zhifeng Yin:** Writing – review & editing. **Fuming Shen:** Formal analysis. **Weizong Weng:** Supervision. **Hao Zhang:** Supervision, Software, Project administration. **Yingying Jiang:** Resources, Data curation. **Xinru Liu:** Visualization, Validation, Supervision. **Yonghui Deng:** Writing – review & editing, Visualization, Supervision. **Yuan Chen:** Validation, Software, Conceptualization. **Ke Xu:** Resources, Funding acquisition, Conceptualization. **Jiacan Su:** Writing – review & editing, Funding acquisition, Conceptualization.

Acknowledgments

This work was supported by the National Key Research and Development Program of China (No. 82230071); National Natural Science Foundation of China (Nos. 82202674, 82202334); Wenzhou Science and Technology Project (Nos. Y20220178, Y20220016).

Supplementary materials

Supplementary material associated with this article can be found, in the online version, at doi:10.1016/j.cclet.2024.110053.

References

[1] J.N. Katz, K.R. Arant, R.F. Loeser, JAMa 325 (2021) 568–578.
[2] J. Li, W. Zhang, X. Liu, et al., Cell Prolif. 56 (2023) e13518.
[3] F. Motta, E. Barone, A. Sica, C. Selmi, Clin. Rev. Allergy Immunol. 64 (2023) 222–238.
[4] T. Wang, C. He, Cytokine Growth Factor Rev. 44 (2018) 38–50.
[5] J.W. Bijlsma, F. Berenbaum, F.P. Lafeber, Lancet 377 (2011) 2115–2126.
[6] H. Zhang, L. Wang, J. Cui, et al., Sci. Adv. 9 (2023) eabo7868.
[7] P. Kulkarni, A. Martson, R. Vidya, S. Chitnavis, A. Harsulkar, Adv. Clin. Chem. 100 (2021) 37–90.
[8] D.J. Hunter, J.L. Bowden, Nat. Rev. Rheumatol. 13 (2017) 703–704.

[9] A. Nowaczyk, D. Szwedowski, I. Dallo, J. Nowaczyk, Int. J. Mol. Sci. 23 (2022) 1566.
[10] M.P. Hellio Le Graverand-Gastineau, Osteoarthritis Cartilage 17 (2009) 1393–1401.
[11] L. Pang, H. Jin, Z. Lu, et al., Adv. Healthc. Mater. 12 (2023) e2300315.
[12] K. Talavera, J.B. Startek, J. Alvarez-Collazo, et al., Physiol. Rev. 100 (2020) 725–803.
[13] J.E. Meents, C.I. Ciotu, M.J.M. Fischer, J. Neurophysiol. 121 (2019) 427–443.
[14] T. Galindo, J. Reyna, A. Weyer, Pharmaceuticals 11 (2018) 105.
[15] E. Nummenmaa, M. Hämäläinen, L.J. Moilanen, et al., Arthritis Res. Ther. 18 (2016) 185.
[16] L.J. Moilanen, M. Hämäläinen, E. Nummenmaa, et al., Osteoarthritis Cartilage 23 (2015) 2017–2026.
[17] M. Mitrovic, A. Shahbazian, E. Bock, M.A. Pabst, P. Holzer, Br. J. Pharmacol. 160 (2010) 1430–1442.
[18] L.J. Moilanen, M. Hamalainen, L. Lehtimaki, R.M. Nieminen, E. Moilanen, PLoS. One 10 (2015) e0117770.
[19] K.J. Cowan, K. Kleinschmidt-Dorr, A. Gigout, et al., Drug Discov. Today 25 (2020) 1054–1064.
[20] L. Kou, S. Xiao, R. Sun, et al., Drug Deliv. 26 (2019) 870–885.
[21] S. Mehta, T. He, A.G. Bajpayee, Curr. Opin. Rheumatol. 33 (2021) 94–109.
[22] S.G. Antimisiaris, A. Marazioti, M. Kannavou, et al., Adv. Drug Deliv. Rev. 174 (2021) 53–86.
[23] X. Ji, Y. Yan, T. Sun, et al., Biomater. Sci. 7 (2019) 2716–2728.
[24] D. Zhou, F. Zhou, S. Sheng, et al., Drug Discov. Today 28 (2023) 103482.
[25] X. Xue, Y. Hu, S. Wang, et al., Bioact. Mater. 12 (2022) 327–339.
[26] J. Yang, Y. Zhu, F. Wang, et al., Chem. Eng. J. 400 (2020) 126004.
[27] Q. Yang, Y. Wang, T. Liu, et al., ACS Nano 16 (2022) 18366–18375.
[28] Z. Xu, G. Liu, P. Liu, et al., Acta Biomater. 147 (2022) 147–157.
[29] R. Ziadlou, S. Rotman, A. Teuschl, et al., Mater. Sci. Eng. C Mater. Biol. Appl. 120 (2021) 111701.
[30] G. Li, S. Liu, Y. Chen, et al., Nat. Commun. 14 (2023) 3159.
[31] C. Shen, J. Wang, G. Li, et al., Bioact. Mater. 35 (2024) 429–444.
[32] Y. Tao, Y. Chen, S. Wang, et al., Compos. Part B: Eng. 247 (2022) 110288.
[33] H. Daraee, A. Etemadi, M. Kouhi, S. Alimirzalu, A. Akbarzadeh, Artif. Cells Nanomed. Biotechnol. 44 (2016) 381–391.
[34] Z. Zhou, P. Song, Y. Wu, et al., Mater. Horiz. 11 (2024) 1465–1483.
[35] E. Nummenmaa, M. Hämäläinen, A. Pemmari, et al., Int. J. Mol. Sci. 22 (2020) 87.
[36] S. Yin, L. Zhang, L. Ding, et al., J. Inflamm. 15 (2018) 27.
[37] T. Ohtsuki, O.F. Hatipoglu, K. Asano, et al., Int. J. Mol. Sci. 21 (2020) 3140.
[38] M.Y. Ansari, N. Ahmad, T.M. Haqqi, Biomed. Pharmacother. 129 (2020) 110452.
[39] W. Hu, Y. Chen, C. Dou, S. Dong, Ann. Rheum. Dis. 80 (2021) 413–422.